Characterization of IL-1 inhibitory factor released from human alveolar macrophages as IL-1 receptor antagonist. *Clin Exp Immunol* 1992;88:181–187.
23. Muller-Quernheim J, Pfeifer S, Mannel D, Strausz J, Ferlinz R. Lung-restricted activation of the alveolar macrophage/monocyte system in pulmonary sarcoidosis. *Am Rev Respir Dis* 1992;145:187–192.
24. Yamaguchi E, Okazaki N, Tsuneta Y, Abe S, Terai T, Kawakami Y. Interleukins in pulmonary sarcoidosis. Dissociative correlations of lung interleukins 1 and 2 with the intensity of alveolitis. *Am Rev Respir Dis* 1988;138:645–651.
25. Abdel-Dayem HM, Scott A, Macapinlac H, Larson S. Tracer imaging in lung cancer. *Eur J Nucl Med* 1994;21:57–81.

Technetium-99m-MIBI in Primary and Recurrent Head and Neck Tumors: Contribution of Bone SPECT Image Fusion

Thomas Leitha, Christoph Glaser, Martha Pruckmayer, Michael Rasse, Werner Millesi, Susanna Lang, Christian Nasel, Werner Backfrieder and Franz Kainberger

University Clinics of Nuclear Medicine, Maxillofacial Surgery, Radiology and Pathology, Department of Biomedical Engineering and Physics, Vienna, Austria

We prospectively investigated 200 patients with the clinical suspicion for head and neck tumors. The final diagnoses were 94 primary and 56 (37 confirmed, 19 excluded) recurrent squamous cell carcinomas (SCCs), 3 primary and 7 (4 confirmed, 3 excluded) recurrent adenoid cystic carcinomas (ACCs), 6 non-Hodgkin's lymphomas, 10 distant metastases, 6 other malignancies, 10 inflammatory and 8 other nonmalignant conditions. **Methods:** Bone (600 MBq ^{99m}Tc-3,3-diphosphono-1,2-propane dicarboxylic acid tetrasodium salt) and hexakis-2-methoxyisobutyl isonitrile (MIBI) (600 MBq ^{99m}Tc-MIBI) SPECT were both performed under identical conditions (triple-head gamma camera; ultra-high-resolution, parallel-hole collimators; three-dimensional postfiltering) and judged independently and after superimposition. The results were compared to the results of biopsy, surgery and CT. **Results:** The overall sensitivity/specificity of MIBI was 90%/78% for tumor detection and 90%/95% for the identification of malignant lymph node involvement (CT: 79%/66%, respectively 90%/79%). In the subgroup of recurrent SCC and ACC the sensitivity/specificity for tumor detection was 95%/71% for MIBI versus 78%/68% for CT. The isolated assessment of bone SPECT had a sensitivity/specificity of 100%/17% for osseous tumor spread. Image fusion of MIBI and bone SPECT differentiated between regio-local bone involvement and inflammatory changes and increased the specificity of bone SPECT to 100% in primary staging. Tumor size, stage, histology and pretreatment had no statistically significant effect on tracer uptake or diagnostic utility of scintigraphy. **Conclusion:** We propose the combined ^{99m}Tc-MIBI and bone ultra-high resolution SPECT as a highly useful imaging approach in the primary and secondary staging in patients with suspected malignancies in the head and neck region. The high specificity for malignancies in the head and neck region may be used in the differential diagnosis between head and neck malignancies and inflammatory disease in patients with the accidental finding of enlarged lymph nodes and no clinical signs of a primary tumor. Image fusion with bone scanning is mandatory for the topographical orientation and increases the specificity of bone scanning to differentiate between inflammatory or malignant causes of increased bone metabolism.

Key Words: technetium-99m-hexakis-2-methoxyisobutyl isonitrile; image fusion; head and neck cancer; bone scan; staging

J Nucl Med 1998; 39:1166–1171

Received Apr. 23, 1997; revision accepted Oct. 13, 1997.
For correspondence or reprints contact: Thomas Leitha, MD, University Clinic Nuclear Medicine, Waehringerguertel 18–20, A-1090 Vienna, Austria.

Cancer of the head and neck accounts for 4%–5% of all cancers in the western world (*1*), with much higher incidences in other areas. Ninety-five percent of the cancers arise from squamous epithelium (SSC) and about 1.5% of head and neck cancers are adenoid cystic carcinomas (ACCs) that arise mainly from the minor salivary glands. Lymphomas account for 1.5% of cases of head and neck cancer. The remaining 2% of cancers of the head and neck are melanomas, soft-tissue tumors and thyroid and parathyroid tumors.

Limited cancer stages, especially in the oral cavity, are accurately assessed by clinical evaluation but tumor depth is clinically underestimated in more advanced stages (*2*). Additionally, in a prospective evaluation of 81 consecutive patients, 17% of multiple primary lesions were clinically overlooked (*3*). The use of the appropriate imaging technology depends on the availability, expertise and experience of the radiologist and on the quality of the equipment available (*4*). The advantages of CT include (a) better sensitivity to bone destruction; (b) better delineation of nodal architecture; (c) lower costs; (d) higher availability; and (e) lower rate of claustrophobia. The advantages of MRI include (a) no necessity for iodinated contrast media; (b) less dental artifacts; (c) multiplanar acquisition; (d) detailed imaging of soft-tissue invasion outside the nasopharynx; and (e) retropharyngeal node involvement (*5*). Nevertheless, MRI is hampered in the detection of bone erosion (*6*), which is crucial for planning the extent of surgery. CT remains the gold standard in staging of head and neck tumors in many institutions (*7*), including ours.

Despite advances in surgical technique and adjuvant radiochemotherapy, recurrent disease ultimately develops in about half of patients with squamous cell carcinoma (SCC) and ACC. Morphological imaging techniques are of limited use in the secondary staging of patients with severe anatomical changes after radiotherapy, surgery and flap reconstruction in the mouth floor.

In clinical routine, many patients present with the accidental finding of enlarged lymph nodes in the head and neck region. In the absence of visible pathologies of the mucosa, the differential diagnosis has to be made between an occult but advanced primary tumor (most likely in the diagnostic cold spot of the nasopharynx), systemic malignancies or inflammatory lymph node enlargement.

At present, nuclear medicine plays only a limited role in the

TABLE 1
Diagnoses of 200 Consecutive Patients with the Clinical Suspicion for Head and Neck Malignancy

No. of patients	Diagnoses	Confirmed/excluded
94	Squamous cell carcinoma: primary	
56	Squamous cell carcinoma: recurrent	37/19
3	Adenoid cystic carcinoma: primary	
7	Adenoid cystic carcinoma: recurrent	4/3
10	Metastases	
8	Lymphoma, AML, plasmocytoma	
4	Sarcoma	
10	Inflammation	
4	Radioosteonecrosis	
3	Benign dentogen tumors	
1	Sarcoidosis	

AML = acute myelogenous leukemia.

staging of head and neck tumors. Recently, metabolic imaging with ^{18}F-fluorodeoxyglucose (FDG) has proved to be useful in primary staging (*8*) and in the detection of tumor recurrence (*9,10*). Unfortunately, PET is a costly technique with limited availability in clinical routine.

Previous attempts with tumor avid tracers have never been accepted in clinical routine and even conventional bone scanning is not universally applied. Because head and neck cancers rarely give rise to bloodborne metastases before regional nodal metastases are evident, only patients with N2 or N3 disease are sent for whole-body bone scanning. Thus, the higher sensitivity of bone SPECT in comparison to CT for assessing osseous tumor spread is not universally used. Another reason for the limited use of bone SPECT in the staging of head and neck tumors is its limited specificity for differential diagnosis of malignant, degenerative or inflammatory changes in patients with inferior dental status.

The combined use of tumor avid tracers and bone scintigraphy should theoretically increase the specificity of bone scanning and additionally provide a better loco-regional staging of primary or recurrent tumor masses. Previous attempts (*11,12*) failed to play a clinical role in the management of head and neck cancer due to the inability to detect low-volume disease because of inferior imaging characteristics of the tumor avid tracer and a low specificity for inflammatory changes for both modalities.

Technetium-99m-MIBI has been successfully applied in oncology and its uptake in malignancies has been found to be not just flow dependent but additionally influenced by certain cellular properties of the tumor, e.g., mitochondria content, membrane potential, invasiveness and epithelial hyperplasia (*13–15*). A preliminary study with ^{99m}Tc-MIBI in nasopharyngeal carcinoma (*16*) reported promising results but did not fully use the possible resolution of a ^{99m}Tc-labeled tracer or high-resolution equipment.

The aim of this study was to investigate the tumor imaging properties of ^{99m}Tc-MIBI in combination with ^{99m}Tc-diphosphonate bone scintigraphy in ultra high-resolution SPECT for the primary and secondary staging of head and neck tumors in comparison to contrast-enhanced CT.

MATERIALS AND METHODS

Patient Selection

Two-hundred consecutive patients (135 men, 65 women; age (mean ± s.d.) 57.4 ± 13.6 yr; median 56) who were referred by the University Clinic of Maxillofacial Surgery as part of the routine work-up of a suspected head and neck tumor were prospectively included in this study. The final diagnoses were based on the histology of guided biopsy or the surgical specimen (Table 1). Cancers of the head and neck were staged according to the tumor-node-metastasis (TNM) system of the American Joint Committee on Cancer (*17*) (Table 2). One hundred thirty-seven patients had no previous history of a head and neck tumor. Sixty-three patients were investigated because of the clinical suspicion for recurrent SCC or ACC. The diameter of the primary tumors ranged from 0.5–12 cm with a median of 3 cm. Ten percent of the tumors were ≤ 1 cm, 32% were ≤ 2 cm. Preceding therapy protocols in patients with recurrent tumors included combined radiotherapy, chemotherapy and surgery in 22, radiotherapy and chemotherapy in 11, radiotherapy and surgery in 7, chemotherapy and surgery in 4, surgery in 12, radiotherapy in 4 and chemotherapy in 3 patients. All patients underwent intravenous contrast-enhanced CT scans, ^{99m}Tc-MIBI and bone scintigraphy within 10 days with at least 72 hr between the two radionuclide studies.

Imaging Studies

Technetium-99m-MIBI Scintigraphy. Ten minutes after the intravenous injection of 600 MBq ^{99m}Tc-MIBI (Cardiolite, DuPont Pharma, Billerica, MA) the patient's head was placed into a shell and taped to allow reproducible positioning. A 360° SPECT (3° angular steps) was performed in all patients using a triple-head gamma camera (PRISM 3000, Picker International, Ohio Imaging Division, Cleveland, OH) equipped with low-energy, ultra-high-resolution collimators over 30 sec per step. A symmetrical 15% window was set at 140 keV and the data were stored in a 128 × 128 matrix. The studies were subjected to ramp-filtered backprojection, three-dimensional postfiltering using a Wiener filter and oblique reformatting into vertical, horizontal long- and short-axis slices.

Technetium-99m-DPD Bone Scintigraphy. Whole-body bone scintigraphy was performed 3 hr after the intravenous injection of 600 MBq ^{99m}Tc-3,3-diphosphono-1,2-propane dicarboxylic acid tetrasodium salt (DPD). Additionally, obtained a SPECT study of the skull was obtained using identical positioning, acquisition and reconstruction algorithms as in the ^{99m}Tc-MIBI study.

CT Imaging. The CT examinations were performed on a spiral CT scanner. Imaging was performed in fast scan technique in the plane parallel to the palatine with intravenous application of 80–120 ml of nonionic iodine contrast agent. Slice thickness was 3 mm with no gap between the slices. In post-therapy patients, the diagnosis was based on sequential studies performed routinely after the end of treatment.

Image Analysis

Normal cranial and cervical ^{99m}Tc-MIBI distribution was determined in patients investigated for hyperparathyroidism (*18*). Any

TABLE 2
Tumor-Node-Metastasis (TNM) Staging and Tumor Site of 94 Patients with Primary Squamous Cell Carcinoma

TNM stage	Total	Oral cavity	Oropharynx	Nasopharynx	Maxillary sinus
Ca in situ	1	1			
T1 N0	14	12	2		
T2 N0	19	16	2	1	
T2 N1	4	4			
T2 N2	2		2		
T3 N0	4	4			
T3 N1	1	1			
T4 N0	24	16	2		6
T4 N1	12	10	1		1
T4 N2	9	5	3		1
T4 N3	4	2			

TABLE 3
Diagnostic Performance of Technetium-99m-MIBI Scintigraphy and Contrast Enhanced CT in Patients with Clinically Suspected Head and Neck Tumors

Target	Sensitivity	Specificity	Accuracy	Wilcoxon test
Tumor				
MIBI	90.3	78.4	86.9	Z = −5.1008 Two-tailed p < 0.0001
CT	78.9	65.9	76.0	
Lymph node				
MIBI	89.7	94.7	93.5	Z = −3.7406 Two-tailed p = 0.0002
CT	89.5	78.8	82.4	
Primary SCC or ACC (n = 97)				
Tumor				
MIBI	90.3	78.4	86.9	Z = −3.0785 Two-tailed p = 0.0021
CT	78.9	65.9	76.0	
Lymph node				
MIBI	89.7	94.7	93.5	Z = −2.0569 Two-tailed p = 0.0397
CT	89.5	78.8	82.4	
Recurrent SCC or ACC (n = 63)				
Tumor				
MIBI	95.3	70.8	86.6	Z = −2.3809 Two-tailed p = 0.0173
CT	78.0	68.0	73.1	
Lymph node				
MIBI	100	94.7	96.8	Z = −1.1531 Two-tailed p = 0.2489
CT	92	94.6	94.0	

SCC = squamous cell carcinoma; ACC = adenoid cystic carcinoma.

other focal tracer retention was considered as abnormal in consensus by two interpreters blinded for clinical information and the results of other imaging studies.

Tumor-to-background (T/B) (area adjacent to the tumor), tumor-to-salivary gland (T/S), tumor-to-nuchal muscles (T/N) and tumor-to-gingival mucosa (T/G) ratios were calculated using regions of interest (ROIs) drawn in consecutive coronal slices in knowledge of the tumor location. T/S and T/G ratios were calculated to assess the tumor uptake in comparison to the regions with physiologically increased tracer retention. The T/N ratio was calculated as a semiquantitative measure for the tumor uptake, assuming a interindividually constant muscle retention of MIBI.

The ^{99m}Tc-DPD studies were assessed in consensus by two interpreters independently from the results of other imaging studies and additionally after image fusion with the ^{99m}Tc-MIBI data. Only corresponding hot spots in both studies were considered to represent malignancy.

Technetium-99m-MIBI and ^{99m}Tc-DPD studies were both acquired on the same equipment and each patient's head was fixed identically in a head shell so corresponding slices of both studies could be superimposed. Technetium-99m-MIBI and CT slices were aligned based on the salivary glands as anatomical landmarks.

Statistical Methods

The original dataset was stored in an Approach (V 3.01, Lotus Development Corp., Munich, Germany) datafile. Statistical calculations were performed using SPSS for Windows (V 5.0.1, SPSS, Inc., Chicago, IL). Uptake ratios between SCC and ACC in the MIBI studies were compared by unpaired Student's t-test. The predictive strength of the different clinical parameters (tumor stage, size, histology and pretreatment regimen) for the MIBI uptake ratios was investigated using forward stepwise logistic regression analysis. The Wilcoxon matched pairs signed rank test was used to compare the results of the MIBI and CT studies in Table 3.

RESULTS

Dental artifacts were noted in 8.5% of the CT studies. The sensitivity, specificity and accuracy of ^{99m}Tc-MIBI SPECT in comparison to the CT is given in Table 3. In essence, MIBI scintigraphy had a significantly higher sensitivity and specificity if applied in patients with a clinically suspected malignancy in the head and neck region, including cases with the final diagnosis of inflammatory conditions and in primary and secondary staging of SCC or ACC, respectively.

The individual tumor stage, size, histology or pretreatment regimen had no statistically significant effect on the diagnostic performance of MIBI scintigraphy. However, due to the limited topographical orientation, the assessment of osseous tumor spread was not possible with sufficient certainty based on the MIBI study alone (Fig. 1). MIBI scintigraphy allowed for a better delineation of tumor borders (Fig. 2) and was also superior to CT in the differential diagnosis of malignant and reactive lymph nodes in patients with the clinical suspicion for a primary tumor. Both methods had an excellent performance for the differential diagnosis of lymph node involvement in tumor recurrences, whereas in certain cases CT underestimated lymph node recurrences (Fig. 3).

The uptake ratios are given in Table 4. No statistically significant differences were observed between SCC and ACC or between primary and recurrent tumor, with the exception that the T/S ratio was significantly higher in recurrent SCC.

The isolated assessment of ^{99m}Tc-DPD bone SPECT revealed true-positive results for osseous tumor spread in 60% of the cases and true-negative exclusion of osseous involvement in 6.9%, respectively. In 11% of the patients, a focal tracer uptake was noted due to nonmalignant causes (e.g., inflammation, degenerative changes). In 22.1% of the patients with a confirmed osseous tumor spread, additional ^{99m}Tc-DPD uptake

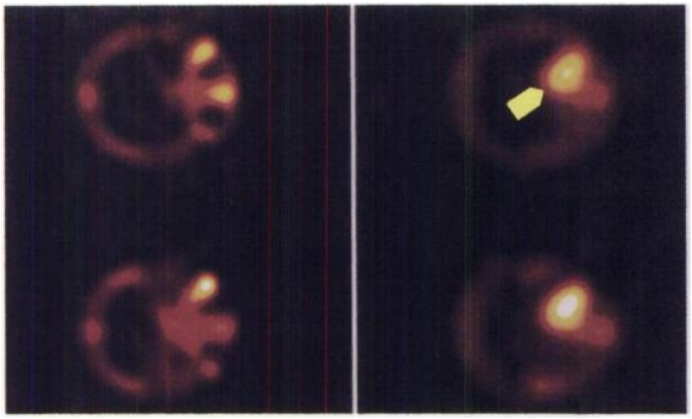

FIGURE 1. A 61-yr-old man with a T4N2M0 G2 SCC originating in the right maxillary sinus (arrow). The ^{99m}Tc-MIBI scans in the upper row show the tumor tissue completely filling the cavity of the right maxillary sinus. The ^{99m}Tc-DPD scans in the lower row clearly delineate osseous infiltration of the lateral and medial wall of the maxillary sinus and allow for better topographical orientation.

was noted in adjacent areas without malignant infiltration. Thus, whereas the sensitivity of the isolated assessment of ^{99m}Tc-DPD bone SPECT for osseous tumor spread was 100%, its specificity was 17.2%.

The combined assessment of the ^{99m}Tc-MIBI and the ^{99m}Tc-DPD studies was able to correctly differentiate osseous tumor spread from nonmalignant causes of increased bone turnover (Fig. 4) except in 3 of 4 cases of suspicious recurrent SCC with radio-osteonecrosis of the mandible. In those 3 patients, a discrete MIBI uptake was noted and consequently those patients were erroneously judged as recurrent tumor. However, the MIBI uptake was significantly less than regional bone uptake.

TABLE 4
Semiquantification of Technetium-99m-MIBI Scintigraphy in Primary and Recurrent Head and Neck Tumors

Ratio	Mean ± s.d.	Median
Tumor:gingival mucosa	1.6 ± 0.9	1.4
Tumor:salivary glands	0.9 ± 1.0	0.7
Tumor:background	5.5 ± 6.7	3.9
Tumor:nuchal muscles	2.5 ± 1.3	2.3

DISCUSSION

Primary Staging of Squamous Cell Carcinoma and Adenoid Cystic Carcinoma

The possible role of diagnostic imaging in patients with suspected head and neck cancer is commonly confined to the imaging of clinical blind spots, e.g., nasopharynx, delineation of advanced cancer, assessment of osseous tumor spread and lymph node staging. We achieved a comparable sensitivity for the primary tumor and malignant lymph node involvement as

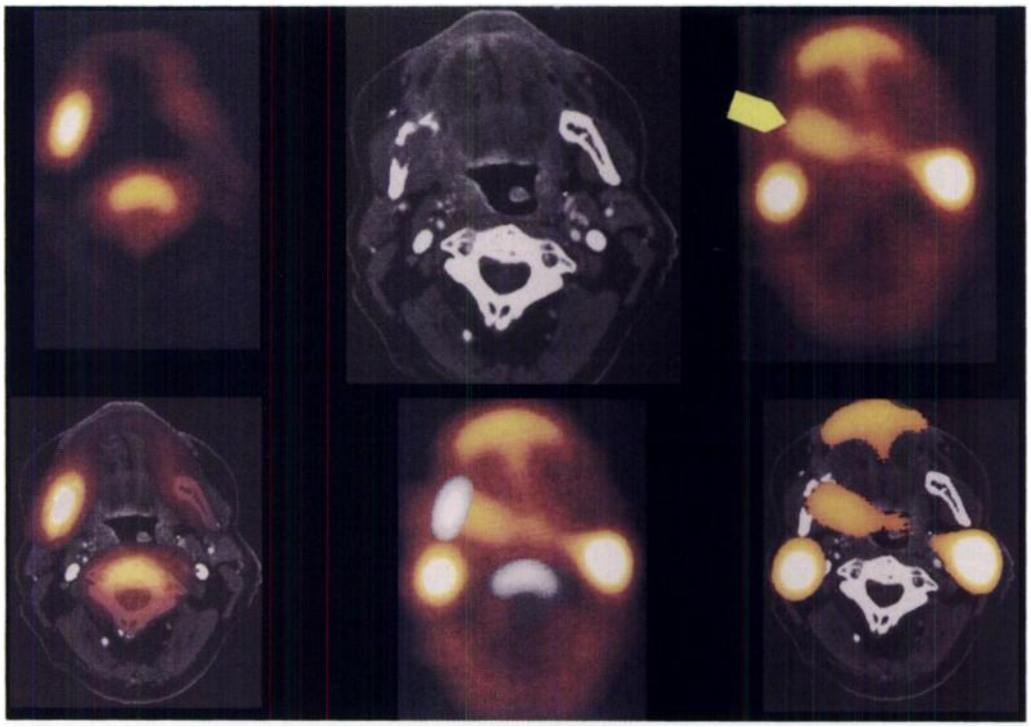

FIGURE 2. A 67-yr-old man with a T4N0M0 G2 SCC originating from the parapharyngeal space and infiltrating the mandible. The ^{99m}Tc-DPD image in the far left of the upper row shows the increased bone turnover in the right mandibular ramus. Contrast-enhanced CT (middle upper row) clearly shows osseous destruction but provides only a faint delineation of the tumor borders. Technetium-99m-MIBI scanning in the far right of the upper row delineates the primary tumor and shows the physiological uptake in the parotid and gingival salivary glands. Osseous tumor spread cannot be assessed with certainty (arrow). The lower row shows (from left to right) image overlay of bone scan and CT, of bone scan and MIBI scan and MIBI scan and CT and confirms osseous tumor spread into the mandible.

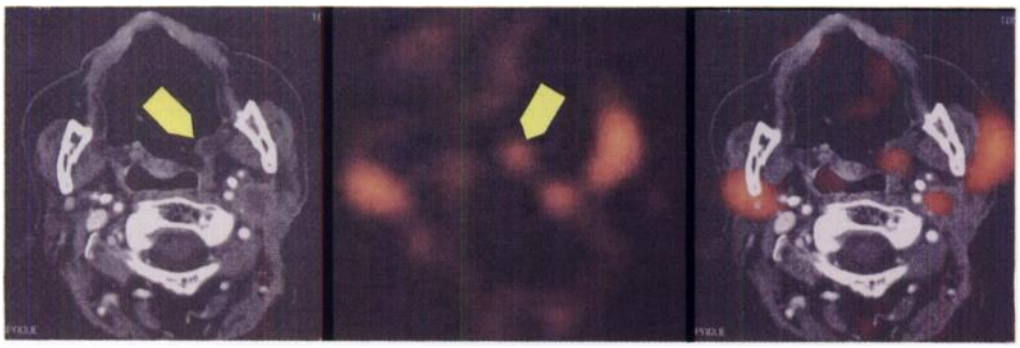

FIGURE 3. Tumor recurrence in a 64-yr-old man 17 mo after resection of a T4N3M1 G2 SCC originating from the tongue. Sequential CT imaging suggested a lymph node recurrence in an enlarged (2-cm diameter) lymph node in the left carotid space but assumed the smaller lymph node (below 1-cm diameter) ventrally (arrow) in the parapharyngeal space to be reactive. However, both lymph nodes showed MIBI uptake and were confirmed to be malignant.

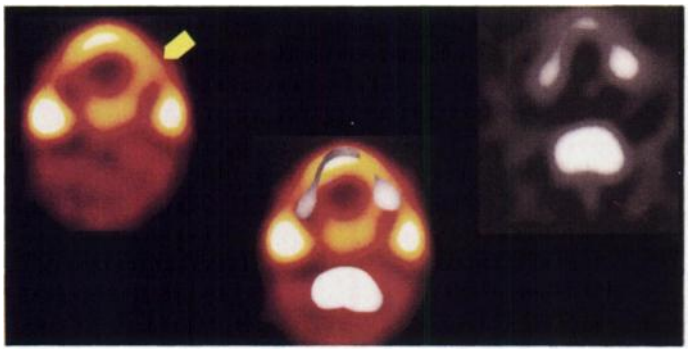

FIGURE 4. Example of a primary T4N1M0 G2 SCC in 38-yr-old man shows utility of ^{99m}Tc-MIBI to increase the specificity of bone scanning. Bone scan in the far right in the upper row shows two areas of focally increased bone turnover bilaterally in the mandible. The ^{99m}Tc-MIBI in the upper row shows the primary tumor extending into the left mandible (arrow). No MIBI uptake was noted adjacent to the focal spot in the right body of the mandible (image overlay in the lower row), which was confirmed to represent periodontitis. The positive submandibular lymph node is outside the displayed planes.

reported recently for high-resolution, dual-head equipment (*19*) and were superior to results with low-resolution systems (*16*). In contrast to others, our study protocol included patients with other primary malignant and nonmalignant conditions that additionally allowed for the assessment of the specificity of MIBI scintigraphy.

Tumor detection with MIBI scintigraphy was significantly superior to CT imaging in patients with a suspected malignancy, but the topographic orientation was difficult for the surgeon without familiar anatomical landmarks. Furthermore, a tumor progression into the osseous structures could only be suspected but not confirmed in the ^{99m}Tc-MIBI scan alone.

The isolated assessment of ^{99m}Tc-DPD bone SPECT had a sensitivity for osseous tumor spread of 100%, confirming the clinical practice that bone-sparing resections of tumors close to the jaw is justified with a negative bone scan (*20*). The inferior dental status of the majority of the patients with SCC and the consecutively high prevalence of periodontitis and other inflammatory conditions decreased the specificity of isolated bone scanning to 17.2% or, in other words, osseous tumor spread could be excluded in only 6.9% of the patients based on the ^{99m}Tc-DPD scan alone.

The combined assessment of the ^{99m}Tc-MIBI and the ^{99m}Tc-DPD studies was able to correctly differentiate osseous tumor spread from nonmalignant causes of increased bone turnover (e.g., dental infections, osteomyelitis, etc.) in all patients during the primary staging. As reported previously, an unspecific periostal reaction in the mandible adjacent to a SCC in the mouth floor may be visualized as hot spot in bone SPECT. If bone scintigraphy is assessed without image fusion with a tumor avid tracer, the tumor stage is overestimated and the patient is unnecessarily subjected to extensive and mutilating surgery (*21*).

In some patients, particularly those with the primary tumor in the nasopharynx, the tumor may be missed clinically and the only presenting feature is lymph node enlargement. If diagnostic imaging excludes an occult primary, the possible differential diagnoses comprise other systemic malignancies or inflammatory lymph node enlargement. Therefore, we investigated the diagnostic utility of ^{99m}Tc-MIBI scintigraphy for the differential diagnosis between other malignancies and nonmalignant head and neck tumors and lymph node enlargements.

Other Malignancies, Differential Diagnosis of Inflammatory and Malignant Lymph Node Enlargement

MIBI scintigraphy was helpful in the differential diagnoses between malignant and benign conditions and should be used as decision tool for guided biopsy. Four of five lymphomas, all distant metastases (breast, colon and pancreatic cancers) and all sarcomas showed a focal MIBI uptake. However, one case with plasmocytoma was missed.

In contrast, inflammatory conditions and lymph node enlargement, e.g., soft-tissue inflammation, viral infection, osteomyelitis, abscesses and sarcoidosis showed no tracer enhancement. Two more patients with sarcoidosis were imaged in our institution out of this protocol and showed no MIBI uptake in enlarged lymph nodes in spite of positive ^{67}Ga-citrate scans. However, this is in contrast to others who reported faint MIBI uptake in hilar sarcoidosis (*22*).

Secondary Staging of Squamous Cell Carcinoma and Adenoid Cystic Carcinoma

Anatomical imaging is generally hampered in postsurgical patients when the normal anatomical planes are altered by radiotherapy and surgery. MIBI scintigraphy had a significantly higher sensitivity for the detection of tumor recurrence than CT, even if the scintigraphic data were based on a single study, whereas CT interpretation was performed based on sequential images after treatment. Our data confirmed previously reported data (*19*) in a larger group of patients. Image fusion with bone imaging was especially helpful in ACC because its propensity to spread in a perineural fashion leads to an anatomically complex tumor spread and renders topographical orientation more difficult.

The differential diagnosis between soft-tissue inflammation and tumor recurrence was possible in all but one case with a large cervical abscess and a consecutively congested intestinal flap in the mouth floor. A central MIBI uptake in the abscess and an increased uptake in the mouth floor was falsely diagnosed as tumor recurrence.

The apparently low affinity of MIBI to inflammatory tissues in the head and neck region in our study is in contrast to the findings in other body regions, e.g., the brain (*23*) or breasts (*24*). Furthermore, a recently updated summary of noncardiac MIBI uptake (*25*) mentioned several inflammatory conditions with focal MIBI uptake. Nevertheless, abnormalities of membrane potentials and a high mitochondrial content have been reported for many tumor-cell types and it has been shown that the cellular MIBI uptake is dependent on mitochondrial content and membrane potentials of the target cell (*26*). We assume that the comparatively high inherent specificity of MIBI for differentiating malignant from inflammatory tissues is masked by the high blood flow and consequently high tracer delivery in most regions of the trunk. Conversely, the lower blood flow in lymph nodes or other structures in the head and neck region may reveal these tumor specific properties of the MIBI kinetics and may account for the higher specificity of MIBI for malignancies in this region.

Nevertheless, the crucial differential diagnosis between radio-osteonecrosis or tumor recurrence was not possible in our study. Whereas, retrospectively, MIBI uptake was consistently lower than DPD uptake in radio-osteonecrosis, adhering to the working hypothesis that any MIBI uptake outside the physiological distribution has to be considered malignant, three of four cases were judged as false-positive.

Semiquantification

Therapy had no statistically significant effect on tracer uptake. The higher T/S in the post-therapy group is most likely

due to a lower tracer uptake in the irradiated salivary gland. Our data show that the physiological gingival uptake can be quantitatively differentiated from tumor uptake. The almost identical uptake of the tumor and the salivary glands hampers the delineation of tumor borders adjacent to the salivary and parotid glands. Small lymph nodes adjacent to the salivary glands cannot be diagnosed from the scan alone, due to the limited resolution of scintigraphy. Asymmetrical tracer uptake in the submandibular region necessitates the comparison with sonography or contrast-enhanced CT. If lymph nodes adjacent to a submandibular gland with an asymmetrically increased uptake can be identified by radiological methods, they are most likely malignant, regardless of the radiological interpretation of their size and tissue structure. Asymmetrically decreased uptake in a submandibular gland is often caused by duct obstruction by the primary tumor.

CONCLUSION

We propose ^{99m}Tc-MIBI scintigraphy as a highly useful imaging modality in patients with suspected malignancies in the head and neck region if a high resolution imaging protocol is used. The high specificity for malignancies in the head and neck region may be used in the differential diagnosis between head and neck malignancies and inflammatory disease in patients with the accidental finding of enlarged lymph nodes and no clinical signs of a primary tumor.

In patients with a confirmed SCC or ACC ^{99m}Tc-MIBI scintigraphy allows a multi planar delineation of the tumor extent even in post-therapy patients. Image fusion with bone scans in patients with positive ^{99m}Tc-MIBI scintigraphy is mandatory for the topographical orientation and increases the specificity of bone scanning to differentiates between inflammatory or malignant causes of increased bone metabolism. It remains to be determined prospectively if a quantitative approach to the differential diagnosis of radiooosteonecrosis and tumor recurrence may be helpful.

REFERENCES

1. Silverberg E, Lubera J. Cancer statistics. *CA Cancer J Clin* 1987;37:2–19.
2. Dillon WP, Harnsberger HR. The impact of radiologic imaging on staging of cancer of the head and neck. *Semin Oncol* 1991;18:64–79.
3. Mc Guirt WF, Matthews B, Koufman JA. Multiple simultaneous tumors in patients with head and neck cancer. *Cancer* 1982;50:1195–1199.
4. Harnsberger HR. *Handbook of head and neck imaging*, 2nd ed. St. Louis, MO: Mosby; 1995.
5. Olmi O, Fallai C, Colagrande S, Giannardi G. Staging and follow-up of nasopharyngeal carcinoma: magnetic resonance imaging versus computerized tomography. *Int J Radiat Oncol Biol Phys* 1995;32:798–800.
6. Tan EL, Chua SL, Kwok R. Use of magnetic resonance imaging in the evaluation of nasopharyngeal cancer. *Ann Acad Med Singapore* 1993;22:720–723.
7. Madison MT, Remley and staging of head and neck squamous cell carcinoma. *Radiol Clin North Am* 1994;32:163–181.
8. Laubenbacher C, Saumweber D, Wagner-Manslau C, et al. Comparison of flourine-18-fluorodeoxyglucose PET, MRI and endoscopy for staging head and neck squamous-cell carcinomas. *J Nucl Med* 1995;36:1747–1757.
9. AnzaiY, Carroll WR, Quint DJ, et al. Recurrence of head and neck cancer after surgery or irradiation: prospective comparison of 2-deoxy-2[^{18}F]fluoro-D-glucose PET and MR imaging diagnoses. *Radiology* 1996;200:135–141.
10. Lapela M, Grenman R, Kurki T, et al. Head and neck cancer: detection of recurrence with PET and 2-[^{18}F]fluoro-2-deoxy-D-glucose. *Radiology* 1995;197:205–211.
11. Fukumoto M, Yoshida S, Yoshida D, Kishimoto S, Dual-isotope SPECT of skull-base invasion of head and neck tumors. *J Nucl Med* 1995;36:1740–1746.
12. Edling CJ. Oberservations on the sequential use of ^{99m}Tc phosphonate and ^{67}Ga imaging in untreated primary and secondary malignant tumors of the head and neck. *Clin Nucl Med* 1983;8:107–111.
13. Arbab AS, Koizumi K, Toyama K, Araki T. Uptake of technetium-99m-tetrofosmin, technetium-99m-MIBI and thallium-201 in tumor cell lines. *J Nucl Med* 1996;37:1551–1556.
14. Piwnica-Worms D, Rao VV, Kronauge JF, Croop JM. Characterization of multidrug resistance P-glycoprotein transport function with an organotechnetium cation. *Biochemistry* 1995;34:12210–12220.
15. Maublant J, de-Latour M, Mestas D, et al. Technetium-99m-sestamibi uptake in breast tumor and associated lymph nodes. *J Nucl Med* 1996;37:922–925.
16. Kao CH, Wang SJ, Lin WY, Hsu CY, Liao SQ, Yeh SH. Detection of nasopharyngeal carcinoma using ^{99m}Tc-methoxyisobutylisonitrile SPECT. *Nucl Med Commun* 1993;14:41–46.
17. American Joint Committee on Cancer. *Head and neck sites: lip and oral cavity. Manual for staging of cancer*, 2nd ed. Philadelphia: JB Lippincott; 1983:25–183.
18. Staudenherz A, Abela C, Niederle B, et al. Comparison and histopathological correlation of three parathyroid imaging methods in a population with ah high prevalence of concomitant thyroid disease. *Eur J Nucl Med* 1997;24:143–149.
19. Kostakoglu L, Uysal U, Özyae E, et al. Pre- and post-therapy thallium-201 and technetium-99m-sestamibi SPECT in nasopharyngeal carcinoma. *J Nucl Med* 1996;37:1956–1962.
20. Fischer-Barndies E, Seifert C. Bone scintigraphy: an aid in deciding on the extent of bone resection in malignant oral tumors. *J Oral Maxillofac Surg* 1995;53:768–770.
21. Glaser C, Pruckmayer M, Staudenherz A, Rasse M, Lang S, Leitha T. Additional diagnostic utility of ^{99m}Tc-sestamibi in the assessment of osseous tumor spread. *J Nucl Med* 1996;37:1526–1528.
22. Aktolun C, Bayhan H. Technetium-99m MIBI in pulmonary sarcoidosis preliminary clinical results and comparison with ^{67}Ga. *Clin Nucl Med* 1994;19:1063–1065.
23. Baillet G, Albuquerque L, Chen Q, Poisson M, Delattre JY. Evaluation of single.photon emission tomography imaging of supratentorial brain gliomas with technetium-99m sestamibi. *E J Nucl Med* 1994;21:1061–1066.
24. Helbich T, Becherer A, Trattnig S, et al. Differentiation of benign and malignant breast lesions: MR-imaging versus ^{99m}Tc-sestamibi scintimammography. *Radiology* 1997;202:421–429.
25. Sutter CW, Stadalnik RC Noncardiac uptake of technetium-99m-sestamibi: an updated gamut. *Semin Nucl Med* 1966;2:135–140.
26. Delmon-Moingeon LI, Piwnica-Worms D, Van den Abbeele AD, Holman L, Davison A, Jones AG. Uptake of the cation hexakis(2-methoxyisobutylisonitrile)-technetium-99m by human carcinoma cell lines in vitro. *Cancer Res* 1990;50:2198–2202.